Design of Experiments Methodology Applied to Satellites Lithium Batteries Aging Modeling

Lorenzo Chapel, Antoine Picot, Fabien Lacressonnière, Didier Loup, Pascal Maussion

Design of experiments methodology applied to satellites lithium batteries aging modeling

Lorenzo Chapel
AIRBUS Defence and Space,
LAPLACE, Université de Toulouse,
CNRS, INPT, UT,
Toulouse, France
chapel@laplace.univ-tlse.fr

Antoine Picot
LAPLACE, Université de Toulouse,
CNRS, INPT, UT,
Toulouse, France
antoine.picot@laplace.univ-tlse.fr

Fabien Lacressonniere
LAPLACE, Université de Toulouse,
CNRS, INPT, UT,
Toulouse, France
fablac@laplace.univ-tlse.fr

Didier Loup
AIRBUS Defence and Space,
Toulouse, France

Pascal Maussion
LAPLACE, Université de Toulouse,
CNRS, INPT, UT,
Toulouse, France
pascal.maussion@laplace.univ-tlse.fr

***Abstract*—This paper is dedicated to the accelerated cycling aging modeling of lithium-ion batteries for satellite applications. Due to the current international context, lifespan of satellites is of dramatic importance. In particular, the impact of the current rate and the depth of discharge on the residual capacity is investigated. The design of experiments methodology is used in order to obtain efficiently the data necessary for modeling. In space applications, numerous are the variables that affect degradation. Notably, the frequency of eclipses and their duration mainly dictates an Earth-orbit satellite battery work schedule according to its mission. Two empirical modeling approaches are tested. The first one is based on a two-parameter power law approach commonly adopted in the literature. A second and new model is then proposed in order to improve in prediction accuracy the previous one. This original work is achieved thanks to the separation of the degradation contributions on the total aging.**

Keywords—Lithium-ion battery, Design of experiments, Aging modeling, Space applications

I. INTRODUCTION

Lithium-ion batteries have been the standard for satellite energy storage since 1992, thanks to their high energy density and reliability [1]. The satellite battery alternates between charging and resting in sunlight, and discharging during eclipses, according to the satellite's operational profile [2]. In particular, an eclipse occurs when the Earth is between the sun and the satellite. The cycling profile is determined by orbit parameters and mission requirements. Orbit parameters, such as altitude and inclination are decided according to the type of mission assigned to the satellite. The most common missions involve for example applications in observation, navigation, telecommunications, and military defense. Three categories of satellites can be therefore distinguished: Low Earth Orbit (LEO), Medium Earth Orbit (MEO) and Geostationary Earth Orbit (GEO) [3].

Despite their excellent performance, Li-ion batteries degrade over time (calendar aging) and with use (cycling aging), through a variety of physical and chemical mechanisms [4–6]. A common indicator to quantify the battery residual capacity is its State of Health (*SoH*), defined as the ratio between its actual and initial capacity value.

In order to assess the battery *SoH*, model-based analysis is often chosen as a prediction and estimation tool [7]. These models can be based on empirical or physical (electrochemical) approaches, or hybrids such as Electrical Equivalent Circuit Models (ECM) [7–10]. In particular, empirical models derive simple algebraic equations from fitting the relationship of various factors onto the data. The complexity and cost of the aging tests necessary for modeling make Design of Experiments (DoE) methodology essential for fast, efficient, multi-factor studies [11].

In order to contribute to the scientific community's efforts and meet industrial needs, the purpose of this original work is to model the impact of the Current rate C_{rate} and the Depth of Discharge *DoD* on the *SoH* with a DoE. The C_{rate} describes the electric current flowing in (or from) the cell compared to its initial capacity. The *DoD* is the percentage of discharged capacity compared to a reference capacity (for this study, its initial capacity). These two factors are key to satellite battery aging modeling since they greatly depend on the mission and strongly impact the battery lifespan.

This paper is organized as follows. Section II introduces the DoE methodology, explains the experimental campaign and presents the first model employed. Section III shows the experimental aging data and the modeling results. In addition to that, the proposition of an alternative modeling approach and relative results are presented. Finally, conclusions and outlooks are discussed in Section IV.

II. METHODS AND MATERIALS

A. Design of experiments methodology

The Design of Experiments (DoE) methodology consists in the careful planning of any collection of experimental runs that aims to answer a specific scientific question. The statistical basis on which this rigorous methodology is built allows the generation of the data necessary to draw solid conclusions with the minimal investment of time, money and resources. The objective of a modeling study is to obtain a mathematical function, a model, that describes a response as a function of several independent factors [12]. The independent factors and respective values, called levels, define a

multidimensional design space. In particular, each factor corresponds to a dimension and its low and high levels define its limits. The experimental design dictates how the experimental runs, called tests, will be placed in this multidimensional space. Several experimental designs suitable for modeling exist, each one with its advantages and inconvenients. Two groups can be distinguished: classic designs and computer-generated designs. Classic designs are preferable since they guarantee orthogonality and balancing between factors and their combinations [13]. Nonetheless, if they require too many tests or if the design space is constrained, computer-generated designs are a valid alternative [14].

A general first-degree polynomial used for most models has this form:

$$y = \beta_0 + \sum_{i=1}^{k} \beta_i x_i + \sum_{i=1}^{k-1} \sum_{j=i+1}^{k} \beta_{ij} x_i x_j + \varepsilon \qquad (1)$$

where y is the response, x_i are the factors (usually normalized between -1 and +1), β_0 is the coefficient of the intercept (corresponding to the average value); β_i are the first order coefficients, corresponding to each factor's contribution; β_{ij} are the two-way interaction coefficients; ε is the random error. It is important to highlight that the model is still linear in the coefficients. Their computation can therefore be handled as a multidimensional linear regression problem. β are usually called regressors of the model. The random error ε describes the discrepancy between the observed values y and the model predicted values. Its origin may derive from human error, factors not considered, measurement noise, dispersion, etc. Due to these uncontrolled and unknown contributions, each regressor β is a statistical entity, to which an expected value and variance (variation around its expected value) are associated. The model is therefore an estimated model, expressed in matrix notation as in:

$$\hat{\boldsymbol{y}} = \boldsymbol{X}\hat{\boldsymbol{\beta}} \qquad (2)$$

where $\hat{\boldsymbol{y}}$ is the vector containing the estimated response values; $\boldsymbol{X}$ is the matrix containing the values of the normalized factors and their combination, it is called design matrix; $\hat{\boldsymbol{\beta}}$ is the vector containing the estimates of the regressors β, also called estimators $\hat{\beta}$. If the number of estimators $\hat{\beta}$ coincides with the number of tests y used to train the model, it is possible to compute $\hat{\boldsymbol{\beta}}$ through matrix inversion. In this case, however, there are no residual degrees of freedom left to quantify the variance $Var(\boldsymbol{\varepsilon})$, unless duplicates or additional tests are included in the system of equations. On the other hand, if the system is overdetermined, it is necessary to use the least square method in order to identify the best fitting estimators $\hat{\beta}$.

B. Design of experiments planning

The impact of the C_{rate} and *DoD* on the *SoH* during cycling aging will be modeled in order to predict the satellites batteries lifespan. In particular, for this study the values of C_{rate} are the same in charging and discharging mode. The choice of the levels will therefore be made in order to build a versatile model for different missions. For each factor, 3 levels are considered in order to observe possible non-linear behaviors. Given 2 the number of factors and 3 the number of levels, it is possible to test every possible combination with a fair amount of resources: 9 tests (3^2) in total. This design approach is called full factorial. The *DoD* window was chosen wide enough to enlarge the validity domain of the model. The low level, 20% *DoD*, is close to LEO applications. The intermediate level, 55% *DoD*, is close to GEO applications. The high level, 80% *DoD*, is chosen in order to test more stressful conditions and eventually consider their practical applicability. Since it is observed that the *DoD* has an exponential impact on the *SoH*, its intermediate value is slightly towards the high values in order to facilitate the linear regression on this factor. Concerning the C_{rate}, the low level, 0.5C, is commonly used in GEO applications. The higher levels, 0.75C and 1C, are employed to accelerate aging. Lower values would have extended the duration of the tests too much. Through extrapolation, it is still possible to make cautious assumptions about aging at lower C_{rate} and *DoD*. The cycling environmental temperature (*T*) and the End of Charge Voltage (*EoCV*) are defined and constant for all cycling phases. They have the following values respectively: *T* 25°C and *EoCV* 4.15V. Only one cell is tested for each condition, for resource availability reasons. To address statistical variability, a new experimental campaign has been initiated to replicate multiple end-of-life profiles under identical conditions. The resulting data will allow a quantitative assessment of model robustness and repeatability in future work. The end of life is considered reached when the cell is no longer capable of supplying the Ampere-hours requested (the defined *DoD*) during the discharge mode. This lack of analysis is compensated by the fact that the studied cells were already tested numerous times in our laboratory and the reproducibility was always demonstrated in satellite battery nominal conditions. Fig. 1 helps visualize in the 2-dimensional design space the position of the tests with untransformed and normalized coordinates.

C. Cycling aging model

The first aging model tested in this paper is the following power law:

$$SoH = 100 - A * FEC^B \qquad (3)$$

where the number of cycles is converted in Full Equivalent Cycles (*FEC*). One *FEC* corresponds to one full charge and one full discharge (100% *DoD*). This scale allows to compare different aging profiles where different cycles correspond to different *DoD*. In the majority of the battery *SoH* modeling studies, the value of *B* is defined and kept constant [8], and only the parameter *A* is then further modelled. The modeling of the parameter *A* as a function of the factors can takes many forms, but similar approaches can be recognized in the literature. The impact of *T* on the *SoH* is often modeled with an Arrhenius law. The C_{rate} is often proven to be strongly interdependent with the temperature. In fact, it is usually modeled as linear at low temperatures and exponentially at higher values. Higher values of *SoC* and *DoD* contributes to higher loss of *SoH*, again with an exponential relationship [4]. For the present study, the aforementioned simplification is not possible due to the observed data behavior heterogeneity: both sublinear ($B<1$) and superlinear ($B>1$). Therefore, both *A* and *B* are initially fitted without constraints with (3). All the 9 aging profiles can be effectively fitted with this simple law.

This first step ensures the coherent monotonic decrease of the model across the whole *FEC* range. In order to describe the values of *A* and *B* for each test as a function of C_{rate} and *DoD*, at least 4 tests are necessary to resolve the system of equations (2). The remaining 5 tests can be used subsequently to validate the resulting model. In order to retain the full factorial design properties of orthogonality and level/center/two-way interaction balance, it is common practice to train the model with the 4 corners of the square in Fig.1 (tests 1, 3, 7, 9) [15]. This system of equations to compute *A* can be made explicit according to equation (2) as follow:

$$\begin{bmatrix} A_1 \\ A_3 \\ A_7 \\ A_9 \end{bmatrix} = \begin{bmatrix} 1 & -1 & -1 & 1 \\ 1 & 1 & -1 & -1 \\ 1 & -1 & 1 & -1 \\ 1 & 1 & 1 & 1 \end{bmatrix} \begin{bmatrix} \hat{\beta}_{0A} \\ \hat{\beta}_{C_{rate}A} \\ \hat{\beta}_{DoDA} \\ \hat{\beta}_{C_{rate},DoDA} \end{bmatrix} \quad (4)$$

Where the design matrix $\boldsymbol{X}$ contains in the first column the normalized values of the intercept, in the second and third the normalized values of C_{rate} and *DoD* respectively and in the fourth their interactions. Through matrix inversion of the system of equations (4), it is possible to compute the estimators $\hat{\beta}_{0A}$ (intercept), $\hat{\beta}_{C_{rate}A}$ and $\hat{\beta}_{DoDA}$ (first order) and $\hat{\beta}_{C_{rate},DoDA}$ (two-way interaction) for *A*. Finally, the parameter *A* can be computed for each factors' combination, hence test, according to equation (1) as follow:

$$A = \hat{\beta}_{0A} + \hat{\beta}_{C_{rate}A} * C_{rate} + \hat{\beta}_{DoDA} * DoD + \hat{\beta}_{C_{rate},DoDA} * C_{rate} * DoD \quad (5)$$

Applying the same approach to *B*, both the model parameters of equation (3) can be described as a function of C_{rate} and *DoD*. The *SoH* for each combination of factors can be therefore computed. Finally, the validity of the resulting model can be verified through various fit metrics.

D. Complementary information

The tested Li-ion cells are commercial high-energy cylindrical 18650 cells with a NMC_{811} (lithium Nickel Manganese Cobalt oxides) positive electrode. The negative electrode is graphite-based and silicon-doped. For reasons of industrial confidentiality, it is not possible to share further information on the cell specifications. All the cells used for the tests belong to the same production batch and no outliers were identified. During this study, for each cell, the residual capacity and the direct current resistance are measured periodically. The *SoH* is computed as the ratio between cell actual and initial discharge capacity value, measured at *C*/5 and 25°C.

III. Results and Discussion

A. Tests results

Fig. 2(a, b, c) present the *SoH* evolution with respect to the *FEC* for the cycling tests. In particular, Fig. 2(a) shows the data for the 3 tests with *DoD* 20%: 1 for each C_{rate}. The same reasoning applies to Fig. 2(b) with *DoD* 55% and Fig. 2(c) with *DoD* 80%. All the tests cycling at *DoD* 20% share the same sublinear aging behavior, which has been observed numerous times for Li-ion cells. According to what has been verified in the literature, it is possible to trace this loss of capacity back to the growth of the Solid Electrolyte Interphase (SEI). For this type of degradation, the values of B usually range from 0.5 to 0.8 since this phenomenon is self-limiting [16]. The coherent increase of degradation with the increase of C_{rate} is also verified. On the other extreme of the spectrum, all the tests cycling at *DoD* 80% share again the same aging behavior, which is this time superlinear. For more stressful conditions, in fact, additional self-reinforcing phenomena such as lithium plating could contribute and induce superlinear aging [17]. The aging trajectories at *DoD* 55% are, on the other hand, far more heterogenous. The test with C_{rate} 0.5C has a constant sublinear behavior. The test with C_{rate} 0.75C starts with a sublinear behavior and after approximately 400 *FEC* changes to a superlinear behavior. Similarly, the test with C_{rate} 1C starts with a sublinear behavior and after approximately 200 *FEC* changes to a linear behavior. This abrupt shift from sublinear to superlinear behavior is commonly called knee. Identifying its inflection point and understanding its root causes is critical for effective predictive modeling [18]. A first hypothesis that can justify these heterogeneous behaviors for the same *DoD* is based on the definition used in this study for this factor. When discharging a percentage of capacity compared to its initial value, the cycling potential window widens with aging and can trigger new threshold side reactions. The dependence of the End of Discharge Voltage (*EoDV*) on the C_{rate} and its evolution towards increasingly lower values may be some of the reasons behind the observed heterogeneous behaviors at 55% *DoD*. Further complementary analyses are necessary in order to make solid hypotheses about the origins of these differences and the arrival of the knee.

B. Classic model results

The methodology presented in Section II is here employed with the model presented in (3). For both *A* and *B*, their untransformed values and their transformation in the natural logarithm scale (and their combinations) are studied in order to improve their modeling. Depending on the scale choice in fact, it is possible to linearize the dependence of *A* and *B* on the factors and thus improve their linear regression. For both *A* and *B*, the natural logarithm scale improves their modeling. In fact, as anticipated in II.*C*, since aging mechanisms are based on chemical reactions, their rate of progression can be modeled according to laws having an exponential form.

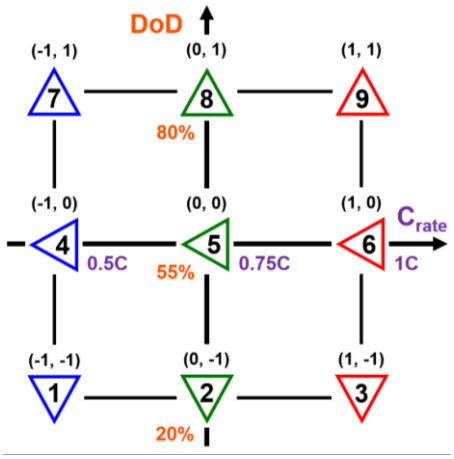

Fig. 1. Full factorial design for 2 factors (C_{rate} and DoD), 3 normalized levels each (-1, 0, 1)

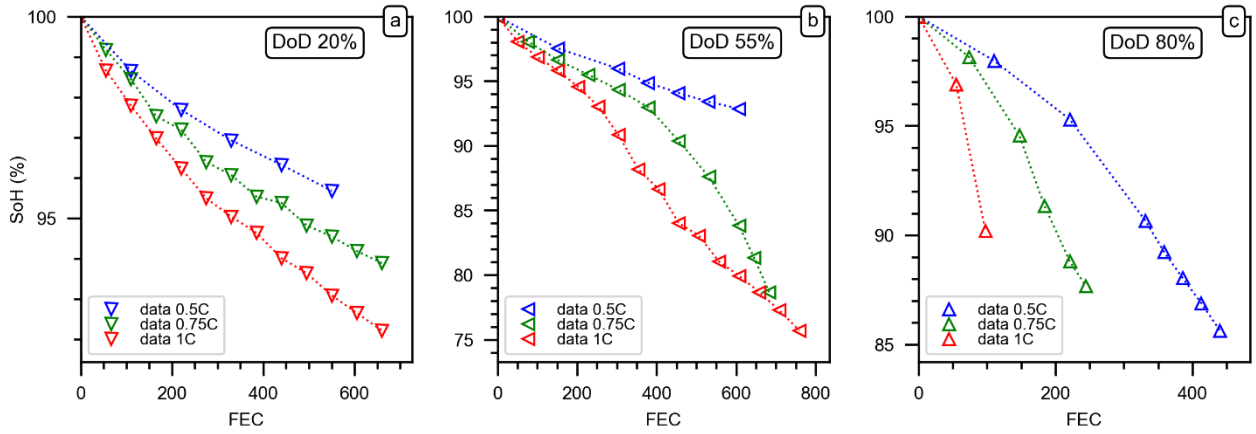

Fig. 2. State of Health (*SoH*) % experimental data evolution with Full Equivalent Cycles (*FEC*) for cycling tests (*DoD* 20% (a), 55% (b) and 80% (c))

Hence, the exponential dependence of these parameters on factors can be linearized in the logarithmic scale. The R^2 and Mean Absolute Percentage Error (MAPE) are used as fit metrics for this study. The first verifies the collinearity of the data and the model. The second, provides a scale-independent relative measure of error. This property is useful in aging studies, since it is important to see the error in proportion to the current SoH value.

This first analysis led to a satisfactory model, with an average R^2 and standard deviation of 0.792 ± 0.156 and with an average MAPE and standard deviation of 1.87 ± 1.22 on the validation tests.

Fig. 3(a, b, c) presents the comparison between experimental data and model predictions. Table I collects the values of R^2 and MAPE for each validation test. It can be observed that the validation tests where the model performs poorly are the ones where the knee appears abruptly after a certain number of *FEC*s (test 5 and 6). By analyzing the estimators' values $\hat{\beta}_0$, $\hat{\beta}_{C_{rate}}$, $\hat{\beta}_{DoD}$ and $\hat{\beta}_{C_{rate},DoD}$, it is possible to quantify the influence of each factor on the degradation parameters *A* and *B*. Concerning the parameter *A*, the impact of the factors is observed to be relatively small, in particular the C_{rate} one. Concerning parameter *B*, *DoD* has the greater contribution. This high dependency of the power *B* on the *DoD* can be visually verified by observing the heterogeneity of the aging behaviors plotted for different *DoD* in Fig. 2(a, b, c).

To conclude, this first modeling approach provides moderate prediction accuracy inside the design limits with relatively low requirements (only 4 tests). In addition to that, it gives an overview of the different factors' contribution to total aging. Such preliminary conclusions allow for quick and reliable screening accelerated studies, an essential part for cell qualification during industrial scouting. Nevertheless, more accurate predictions are needed in order to adapt the battery sizing to the satellite mission and anticipate the possible occurrence of the knee.

C. Separation of degradation dynamics model

As reported in the literature and as can also be seen in the previous model, one of the most complex challenges when modeling cells aging is the knee [18]. In order to address that, a new approach where the different degradation dynamics are modeled separately is proposed. The first step consists in modeling the contribution of the sublinear part of the aging. The second one consists in modeling the residual aging as the superlinear contribution. The shape of this new model can be written as follows:

$$SoH = 100 - A_{sub} * FEC^{B_{sub}} - A_{super} * FEC^{B_{super}} \quad (6)$$

The sublinear behavior can be observed at *DoD* 20%, and at the first *FEC*s of the *DoD* 55% tests. A_{sub} and B_{sub}, the values to model corresponding to the first step, are trained with the tests 1, 2, 4, 5 from Fig. 1. This 2x2 square retains the properties of the initial full design and collects tests where the sublinear behavior is observed. For test 5, only the pre-knee data are fitted. For both A_{sub} and B_{sub}, no transformation in the logarithmic scale was necessary. Now that a model for the sublinear part is computed, it is possible to subtract its contribution from the total aging in order to isolate the superlinear contribution from all the tests. In order to model A_{super} and B_{super}, it is necessary to choose a second training matrix accordingly. In fact, by choosing only tests where the knee is present, the model will not be able to predict the aging where the knee does not occur. Hence a balanced mix between sublinear and superlinear aging profiles must be chosen, while maintaining the properties of the full factorial design, which is not obvious. In order to find the best matrix, the properties and resulting model accuracy of each combination of 4 tests are compared. The combination of tests 1, 2, 7, 8 stands out among all possible matrices. In fact, it is able not only to provide the best accuracy for the full model, but also to retain the mathematical properties of the initial design. For A_{super}, the natural logarithm scale improved the accuracy. For the overall modeling of A_{sub}, B_{sub}, A_{super} and B_{super} only 6 different tests were used (learning set), leaving 3 tests to validate the full model (validation set). Since the tests 2 and 5 contributed only to the first part of the model, it is possible to use them to validate the final model.

This second model improves the *SoH* predictions, with an average R^2 and standard deviation of 0.926 ± 0.088 and with an average MAPE and standard deviation of 0.862 ± 0.857 on the validation tests 3, 4, 5, 6, 9. If only the tests 3, 6, 9 are employed for validation, R^2 0.962 ± 0.036 and MAPE 0.698 ± 0.453 are obtained.

Fig. 3(a, b, c) presents the comparison between experimental data and model predictions. Table I collects the

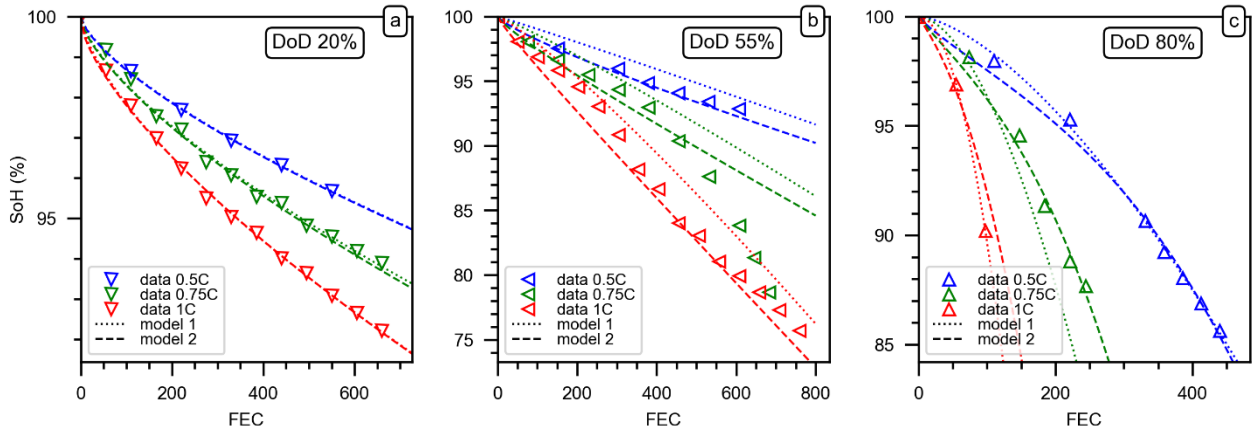

Fig. 3. Results of the first model fit (model 1, equation (3), dotted line) and second model fit (model 2, equation (6), dashed line) to State of Health (*SoH*) % experimental data for cycling tests (*DoD* 20% (a), 55% (b) and 80% (c)) in Full Equivalent Cycles (*FEC*).

values of R^2 and MAPE for each validation test and highlights the improvements over the first model. Even if this model slightly improves the modeling of the knee, an abrupt change in aging behavior is not fully predicted. Concerning the estimators' analysis, with this approach it is possible to highlight the impact of the factors on the two degradation behaviors. In particular, for both A_{sub} and B_{sub}, the *DoD* and C_{rate} participate marginally to the overall degradation. From an electrochemical point of view, these dependencies can be linked to the SEI growth and its decomposition. The C_{rate} facilitates the growth through lithium ions diffusion. The *DoD*, on the other hand, causes fractures in the SEI due to the change in volume of the electrode, providing new growth surfaces for this passivation layer. The most impactful parameters for the SEI growth are time and temperature, both constant factors for this design [19]. This could be the reason why the contributions of C_{rate} and *DoD* are observed to be marginal. Concerning the superlinear behavior, the great *DoD* contribution on both A_{super} and B_{super} suggests that a self-reinforcing phenomenon depending on this factor could be the main cause of the knee. Further complementary analysis is needed to answer that. Interestingly, this second model did not need any test at C_{rate} 1C for the training. This means that testing under closer-to-nominal conditions (more interesting for practical applications) is sufficient to make hypotheses about aging even under hypothetical more stressful conditions. Finally, to assess the model's sensitivity to variations in C_{rate} and *DoD*, its predictions at intermediate values have been tested, indicating physical consistency.

In comparison, this approach increases the prediction accuracy obtained from the first model trained on the 4 corners design. From a practical point of view, that means the addition of a few laboratory tests after a screening campaign is able to improve the first model for more precise aging prediction and to recognize the impact the factors have on the different degradation's behaviors.

IV. Conclusions and Perspectives

In this study, a new and original empirical model has been obtained thanks to a full factorial design of experiments. The impact of the factors C_{rate} and *DoD* has been studied on a commercially available Li-ion cells used in Earth-orbit satellites applications. Two aging models have been tested. The first one, based on a common two parameters approach, provides a simple but reliable prediction model. The small training pool requirements (4 tests), makes it ideal for preliminary studies, such as cell qualification during industrial scouting. A second model is then proposed in order to improve accuracy and study more in detail the impact of the factors on the different degradation behavior of the cell. Mainly sublinear at low stress conditions and superlinear at more stressful ones. This allows to design the size of the battery and its usage schedule according to the impact of these factors on the overall degradation, improving lifespan and reducing costs.

Even if tangible improvements are obtained between the first and second model with a slightly larger training pool (6 tests), the prediction of the sudden onset of the knee is still difficult. More tests are necessary in order to validate more complex models. Including factors' quadratic contributions or additional parameters, such as the knee inflection points, are methods that could improve the accuracy of the model. Finally, if a calendar model is available for the cell, its contribution can be subtracted from the cycling aging in order

TABLE I. Models fit metrics comparison

N.		1	2	3	4	5	6	7	8	9
R^2	**M.1** [a.]	/ [b.]	0.99	/	0.81	0.59	0.92	/	0.64	/
	M.2 [a.]	/	/	1.00	0.98 [c.]	0.76 [c.]	0.98	/	/	0.91
MAPE	**M.1**	/	0.12	/	0.98	3.66	2.26	/	2.33	/
	M.2	/	/	0.08	0.27 [c.]	2.51 [c.]	1.14	/	/	0.88

[a.] M.1: Model 1, equation (3) / M.2: Model 2, equation (6)

[b.] The tests in which the metric values are absent ('/') were employed for the final training of the model

[c.] Tests employed partially to train the sublinear part of the model

to improve its modeling. This is particularly important for accelerated aging tests where the contribution of time is heavily modified.

To conclude, the distinction of the aging contributions has been shown to bring improvements in the modeling. Moreover, the modeled impact of the factors on these degradation behaviors allows for better understanding on the involved electrochemical phenomena. Nonetheless, complementary analysis such as Incremental Capacity Analysis (ICA) and Electrochemical Impedance Spectroscopy (EIS), are necessary to confirm any hypothesis [10] [20].

In perspective, some improvements to this methodology can be made. To verify in depth the predictive power of the presented new model, a series of additional tests under intermediate conditions closer to nominal was recently launched. Concerning the factors studied, while this study focuses on constant *T* and *EoCV* as typically observed in satellite operations, these parameters can vary in flight. Extending the model to include *EoCV* or *T* as additional factors is straightforward from a DoE perspective, but would require more experimental runs or alternative design strategies such as D-optimal or fractional factorial designs. Finally, the integration of Artificial Intelligence and Machine Learning approaches represents a promising way to enhance modeling, automate knee detection, and optimize experimental design in order to reduce manual intervention in the learning phase. In addition to that, the analytical simplicity of the presented new model lends itself well to these applications based on reduced order modeling and physics-based constraints.

ACKNOWLEDGMENT

The authors would like to warmly thank Gwenaëlle Courbaron, Xavier Leturmy, Willy Brevet, Gabriel Beulaguet and Julien Laurent, from Airbus Defence and Space, for their precious help during the experimental campaign and the writing of this paper.

REFERENCES

[1] A.D. Pathak, S. Saha, V.K. Bharti, M.M. Gaikwad and C.S. Sharma, “A review on battery technology for space application”, Journal of Energy Storage, vol. 61, 2023.

[2] Y. Borthomieu, “Satellite Lithium-Ion Batteries”, Lithium-Ion Batteries: Advances and Applications, pp.311-344, 2014.

[3] V. Knap, L. Vestergaard and D. Stroe, “A Review of Battery Technology in CubeSats and Small Satellite Solutions”, Energies, vol. 13, 2020.

[4] W. Vermeer, G.R. Chandra Mouli and P. Bauer, "A Comprehensive Review on the Characteristics and Modeling of Lithium-Ion Battery Aging," IEEE Transactions on Transportation Electrification, vol. 8, 2022.

[5] J. Edge, S. O'Kane, R. Prosser, N. Kirkaldy, A. Patel, A. Hales, A. Ghosh, W. Ai, J. Chen, J. Jiang, S. Li, M. Pang, L. Bravo Diaz, A. Tomaszewska, M. Marzook, K. Radhakrishnan, H. Wang, Y. Patel, B. Wu and G. Offer, “Lithium ion battery degradation: What you need to know”, Physical Chemistry Chemical Physics, vol. 23, 2021.

[6] C.R. Birkl, M.R. Roberts, E. McTurk, P.G. Bruce and D.A. Howey, “Degradation diagnostics for lithium ion cells”, Journal of Power Sources, vol. 341, pp. 373-386, 2017.

[7] S. Ansari, A. Ayob, M.S.H. Lipu, A. Hussain and M.H.M. Saad, “Remaining useful life prediction for lithium-ion battery storage system: A comprehensive review of methods, key factors, issues and future outlook”, Energy Reports, vol. 8, pp. 12153-12185, 2022.

[8] P. Gasper, K. Gering, E. Dufek and K. Smith, “Challenging Practices of Algebraic Battery Life Models through Statistical Validation and Model Identification via Machine-Learning”, Journal of The Electrochemical Society, vol. 168, 2021.

[9] F. Brosa Planella, W. Ai, A.M. Boyce, A. Ghosh, I. Korotkin, S. Sahu, V. Sulzer, R. Timms, T.G. Tranter, M. Zyskin, S.J. Cooper, J.S. Edge, J.M. Foster, M. Marinescu, B. Wu and G. Richardson, “A continuum of physics-based lithium-ion battery models reviewed”, Progress in Energy, vol. 4, 2022.

[10] P. Iurilli, C. Brivio, V. Wood, “On the use of electrochemical impedance spectroscopy to characterize and model the aging phenomena of lithium-ion batteries: a critical review”, Journal of Power Sources, 2021.

[11] L.A. Roman-Ramírez, J. Marco, “Design of experiments applied to lithium-ion batteries: A literature review”, Applied Energy, 2022.

[12] D.C. Montgomery, “Design And Analysis Of Experiments”, 9th ed. USA Wiley, 2017.

[13] G.E.P. Box, K.B. Wilson, “On the experimental attainment of optimum conditions”, J R Stat Soc Series B Stat Methodol, 1951.

[14] R.H. Myers, D.C. Montgomery, C.M. Anderson-Cook, “Response surface methodology: Process and product optimization using designed experiments”, Wiley series in probability and statistics, 2016.

[15] A. Al Haddad, A. Picot, L. Canale, P. Dupuis, G. Zissis and P. Maussion, "Modeling OLED Luminance Decay Under Thermal, Constant and Cyclic Electrical Stress", IEEE Transactions on Industry Applications, vol. 59, 2023.

[16] J. Schmalstieg, S. Käbitz, M. Ecker and D.U. Sauer, "A holistic aging model for Li(NiMnCo)O_2 based 18650 lithium-ion batteries", J. Power Sources, vol. 257, 2014.

[17] F. Todeschini, S. Onori and G. Rizzoni, "An experimentally validated capacity degradation model for Li-ion batteries in PHEVs applications", IFAC Proc. Vols., vol. 45, 2012.

[18] P.M. Attia, A. Bills, F.B. Planella, P. Dechent, G. dos Reis, M. Dubarry, P. Gasper, R. Gilchrist, S. Greenbank, D. Howey, O. Liu, E. Khoo, Y. Preger, A. Soni, S. Sripad, A.G. Stefanopoulou and V. Sulzer, “Review—'Knees' in Lithium-Ion Battery Aging Trajectories”, Journal of The Electrochemical Society, vol. 169, 2022.

[19] A. Wang, S. Kadam, H. Li, S. Shi and Y. Qi, “Review on modeling of the anode solid electrolyte interphase (SEI) for lithium-ion batteries”, npj Comput Mater 4, 15, 2018.

[20] M. Dubarry, D. Anse, “Best practices for incremental capacity analysis”, Front. Energy Res., Sec. Electrochemical Energy Storage, vol. 10, 2022.